

## A Comparative Study of Perturb & Observe and ANN-Based MPPT Algorithms Under Various Environmental Conditions

Mohammed .O. Daw<sup>1\*</sup>, Saleh.M. Shalem<sup>1</sup>, Laith Jaafer Habeeb<sup>2</sup>, Ayoub O . Faraj<sup>1</sup>,  
abdulwahab garboa<sup>3</sup>.

*1 Electrical Engineering Department, Faculty of Engineering, University of Benghazi, Benghazi, Libya.*

*2 Training and Workshop Center, University of Technology- Iraq, 10066 Baghdad, Iraq.*

*3 The Higher Institute of Science and Technology, Elmarej, Libya*

Received: 02 / 02 / 2025 | Accepted: 05 / 10 / 2025 | Publishing: 29/06/2025

### ABSTRACT

This Photovoltaic energy is a promising renewable energy source because it provides a cleaner alternative to fossil fuels. However, the output power of a PV system is affected by factors like solar irradiance and temperature that can change and influence its performance. Therefore, techniques for maximum power point tracking must be developed so the photovoltaic system produces the maximum power. These techniques guarantee that the PV system has the highest power point at all times regardless of weather conditions. The two types of controllers that are presented in this paper are based on the traditional Perturbation and Observation method and the use of artificial neural networks. From simplicity, low cost, and suitability for medium to large photovoltaic systems, the Perturbation and Observation method is chosen. On the other hand, artificial neural networks is well suited to manage complex systems and may assist in improving maximum power point tracking. In addition, the performance of these two methods is compared to a fuzzy logic-based MPPT approach that was developed and published in a previous study. The controllers were evaluated under various environmental conditions using MATLAB/Simulink. The results demonstrated that the artificial neural networks-based controller outperformed both the Perturbation and Observation and fuzzy logic controller methods in terms of efficiency and overall performance. Additionally, the artificial neural networks approach significantly minimized power fluctuations. However, the fuzzy logic controller method showed a faster response in reaching the maximum power point compared to both the artificial neural networks and Perturbation and Observation techniques.

**Keywords:** Artificial Neural Networks, DC-DC Boost converter, MATLAB-Mathematics Laboratory, MPPT, Perturbation and Observation, Solar photovoltaic.

**\*Corresponding Author:** Mohammed .O. Daw, [mohammed.daw@uob.edu.ly](mailto:mohammed.daw@uob.edu.ly)

## 1.INTRODUCTION

The photovoltaic (PV) systems offer a cleaner environment and assist to exploit the economic advantages of the sustainable solar energy and hence promote the production of electricity. These systems are nowadays available and differ, as they have low operation costs, minimal maintenance, and are among the cleanest energy sources. Their main disadvantage is geometry-related low efficiency in turning solar energy into electricity. The PV modules are subject to environmental factors like temperature and sunlight radiation to test their performance<sup>[1]</sup> that impact the amount of energy that is collected in varying weather conditions. Maximum power point (MPP) at which the optimum energy is delivered may therefore be variable depending on solar irradiation and temperature of the solar cells as well as the load conditions<sup>[3,2]</sup>. To accurately track this point, an effective tracker is placed between the PV system and the load. The tracker must be designed for high performance, fast response times, and minimal fluctuations. Due to the unpredictable irradiance and temperature, it is not feasible to connect the load to the PV system directly to obtain maximum

power. Instead, we need a balance of system (BOS), which in general is a DC-DC converter to adapt the load appropriately. The power to the load is delivered effectively using this converter<sup>[4]</sup>. It has been proposed in the literature, many strategies exist to solve this problem, each having different complexity, response time, cost, and type, as well as several sensors needed for hardware implementation<sup>[5-10]</sup>. However, these strategies can generally be divided into two distinct broad categories. The first type of these methods is common traditional methods like Perturb and Observe (P&O) and incremental conductance (IC), etc. Nevertheless, these methods have several shortcomings, including oscillations near the maximum power point and low efficiency upon large irradiance changes. The second type of method used to address these challenges is founded on techniques from artificial intelligence (AI), such as artificial neural networks (ANN) and fuzzy logic. In a previously published study by the authors<sup>[11]</sup>, we proposed we implemented a fuzzy logic-based MPPT controller and assessed its effectiveness under various environmental conditions. The fuzzy logic technique exhibited strong adaptability and rapid con-

vergence to the maximum power point, along with a noticeable reduction in power oscillations. However, it required precise parameter tuning and imposed a relatively high computational burden compared to conventional methods. To further enhance MPPT efficiency while maintaining implementation simplicity, this study investigates and compares two alternative techniques: the conventional P&O algorithm and an ANN-based controller. These methods were implemented and tested under varying irradiance and temperature conditions using MATLAB/Simulink. The results were then compared with those from a previous study by the authors, which

employed a fuzzy logic controller (FLC). The performance of all three techniques was evaluated in terms of tracking efficiency, dynamic response, system complexity reduction, and output stability. Due to its simplicity, the PV module's characteristics are simulated using a one-diode mathematical model of a solar cell. Additionally, a boost-type DC/DC converter is used, chosen for its appropriateness in standalone applications. Therefore Fig.1 illustrates the complete proposed photovoltaic system, which comprises several key components: the PV array, the MPPT algorithms, and the DC/DC boost converter.

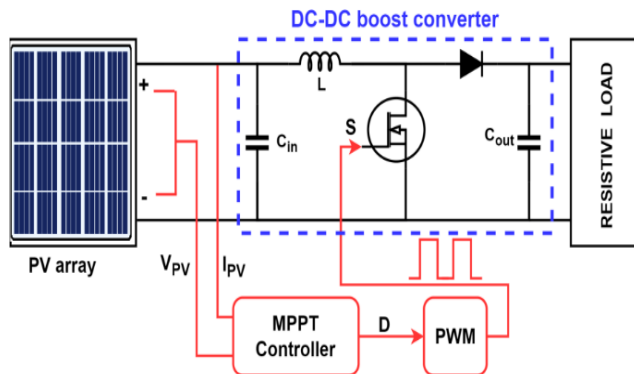


Figure .(1): The complete proposed photovoltaic system

**2.MODELING OF PV ARRAY**

A solar cell is an electrical device that uses the photovoltaic effect to transform light energy into electricity. Figure (2) depicts a single-diode model of the equivalent circuit of a PV cell. This model includes a current source (photocurrent), a diode (D), series resistance, which is responsible for the internal resistance of the current flow, and shunt resistance, which is responsible for the leakage current [7, 12]12

DisplayText<<record><rec-number>41</rec-number><foreign-keys><key app="EN" db-id="svfxzrrzix5dsbe9fe75raa190909t5eev5a" timestamp="1728181661">41</key></foreign-keys> <ref-type name="Journal Article"> 17</ref-type><contributors><authors><author>Al-Majidi, Sadeq D</author><author>Abbod, Maysam F</author><author>Al-Raweshidy, Hamed S</author></authors></contributors><titles><title>A novel maximum power point tracking technique based on fuzzy logic for photovoltaic systems</title><secondary-title>International Journal of Hydrogen Energy</secondary-title></titles><periodical><full-title>International Journal of Hydrogen Energy</full-title></

periodical><pages>14158-14171</pages><volume>43</volume><number>31</number><dates><year>2018</year></dates><isbn>0360-3199</isbn><urls></urls></record></Cite><Cite><Author>Eid</Author><Year>2019</Year><RecNum>70</RecNum><record><rec-number>70</rec-number><foreign-keys><key app="EN" db-id="svfxzrrzix5dsbe9fe75raa190909t5eev5a" timestamp="1749816775">70</key></foreign-keys><ref-type name="Conference Proceedings">10</ref-type><contributors><authors><author>Eid, Mohammed A Elsayed</author><author>Elbaset, Adel A</author><author>Ibrahim, Hamed A</author><author>Abdelwahab, Saad A Mohamed</author></authors></contributors><titles><title>Modelling, simulation of MPPT using perturb and observe and incremental conductance techniques for stand-alone PV Systems</title><secondary-title>2019 21st International Middle East Power Systems Conference (MEPCON) .

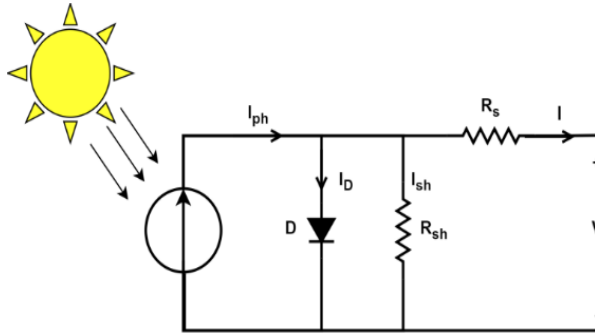


Figure.(2): PV cell equivalent circuit.

Under the condition of solar PV cell being illuminated by solar irradiance, the current output of a cell could be calculated based on Kirchhoff law as shown in Equation 1.

$$I = I_{ph} - I_s - \frac{(V + IR_s)}{R_{sh}} \quad \text{---(1)}$$

The light-generated current is primarily influenced by the sunlight irradiance and the operating temperature of the PV cell, as described in Equation 2.

$$I_{ph} = \left[ I_{sc} + K_i (T - T_{ref}) \right] \cdot \left( \frac{G}{1000} \right) \quad \text{---(2)}$$

The PV saturation current (IS) varies as a cubic function of the temperature (T) of the PV cell, and it is represented in Equation 3.

$$I_s = I_{rs} \left( \frac{T}{T_{ref}} \right)^3 \exp \left[ \frac{q \cdot E_g}{K \cdot A} \cdot \left( \frac{1}{T_{ref}} - \frac{1}{T} \right) \right] \quad \text{---(3)}$$

The reverse saturation current ( I<sub>rs</sub> ) can be roughly calculated using Equation 4.

$$I_{rs} = \frac{I_{sc}}{\left[ \exp \left( \frac{q V_{oc}}{N_{ser} \cdot K \cdot A \cdot T} \right) - 1 \right]} \quad \text{---(4)}$$

Where:

I: Current of PV.

V: Voltage of PV.

I<sub>ph</sub>: The light generated current.

I<sub>s</sub> : The PV saturation current.

I<sub>rs</sub> : The reverse saturation current.

I<sub>sc</sub> : short circuit current.

T : operating temperature of PV module in

kelvin.

Tref : temperature of reference =298K.

Rsh : Shunt resistor of the PV.

Rs: Series resistor of the PV.

A : An ideality factor.

K : Boltzmann constant ( 1.38065003J/K).

G : Solar radiation.

Ki : Short-circuit current temperature coefficient.

Nser : Series number of cells.

Eg : the band gap energy for silicon = 1.1 e V.

q : is the electron charge (1.60217646 C)

A photovoltaic (PV) cell's I-V and P-V characteristics, which show how a PV array typically behaves at different temperatures and sunlight irradiance, affect how much elec-

tricity the cell produces. The I-V and P-V characteristics of a standard PV (MSX-60W) are shown in Figure. (3) are presented at various temperatures, while Fig.4 showcases these characteristics under different levels of sunlight irradiance [2]. The output voltage of a PV system is affected by temperature, typically decreasing as temperatures rise. In contrast, the output current increases linearly with higher solar irradiance, meaning that greater sunlight exposure leads to increased current generation. The P-V curve depicts the relationship between output power (P) and voltage (V), with the maximum power point (MPP) clearly marked. MPP is subject to variation based on weather conditions.

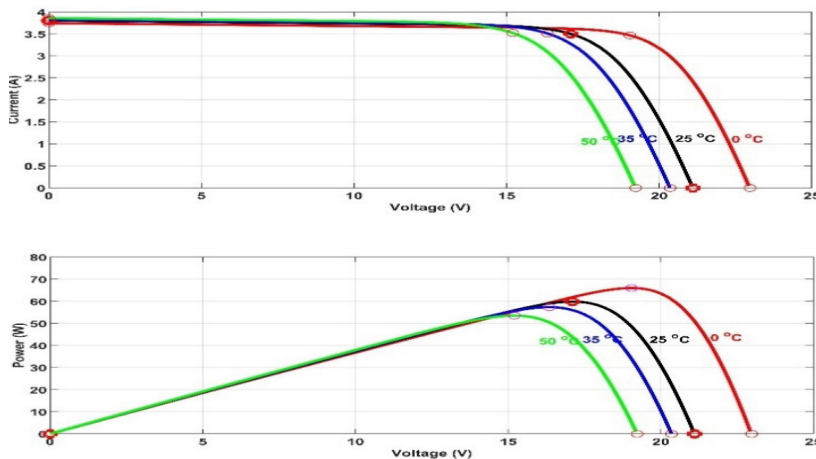
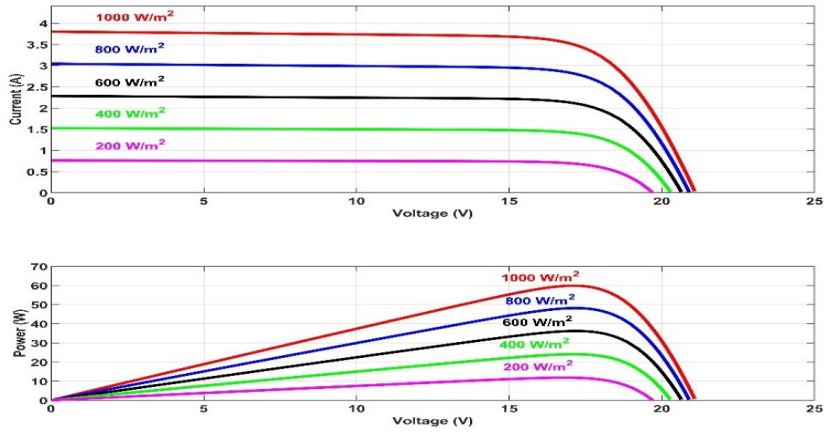


Figure. (3): I-V and P-V characteristics of a typical PV module at various temperatures



**Figure .(4):** I-V and P-V characteristics under different levels of sunlight irradiance.

The parameters for the PV array (MSX60 at 1000 W/m<sup>2</sup> and 25°C) are provided in Table (1).

**Table .(1):** Parameter specification of MXS 60 PV module.

Parameter	Variable	value
Voltage at MPP	VMPP	17.1V
Current at MPP	IMPP	3.5 A
Power at MPP	PMPP	60W
Open circuit voltage	Voc	21.1 V
Short circuit current	Isc	3.8A
coefficient of temperature for short circuit current	Ki	0.06 mA/
total number of cells connected in series	Nser	36
total number of cells connected in parallel	Np	1

### 3.DC-DC BOOST CONVERTER

Connecting a PV panel directly to a load can result in significant power losses due to impedance mismatch. A DC-DC converter with the proper impedance matching is necessary to optimize the PV panel’s power flow to the load. This paper adopts a boost converter and off<sup>[13]</sup>.

verter topology because of its grid connection suitability. A boost converter is so named because it produces an output voltage higher than its input. The circuit shown in Figure. (5) includes an inductor, switch, diode, and capacitor, and works as a switching converter by regularly turning the electronic switch on

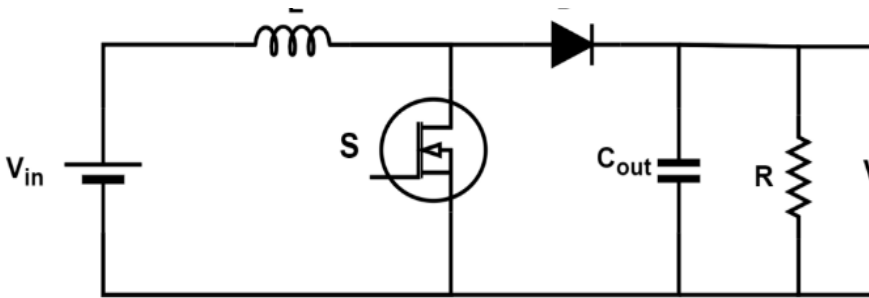


Figure. (5). The circuit diagram of the boost converter

The boost converter has two operation modes. The diode is reverse-biased in the first mode, which allows current to rise and flow to the load via the switch and inductor when the switch is ON. When the switch is off in the second mode the diode is forward-biased and allows the inductor to dump its current into the load through the capacitor<sup>[14, 15]</sup>. The connection between input and output voltage is expressed by Equation 5:

$$\frac{V_{out}}{V_{in}} = \frac{1}{1 - D} \quad \text{--- (5)}$$

Where:

-Vout and Vin: input and output voltages.

-D: duty cycle.

The boost converter’s inductor and capacitor are designed based on the performance requirements of the boost function, with their values calculated using Equations 6 and 7.

$$L = \frac{V_{in} D}{\Delta i L * f_s} \text{---(6)}$$

$$C = \frac{D}{R \left( \frac{\Delta V_o}{V_o} \right) f_s} \text{---(7)}$$

Where:

D is Duty cycle.

$\Delta i L$  is Inductor current ripple.

Output voltage ripple.

$f_s$  is switching frequency.

The design of DC-DC boost converter is shown in Table (2).

**Table .(2):** The designed specifications for the boost converter

Parameter	Symbols	values
Input capacitor (uf)	Cinp	225
Output capacitor (uf)	Cout	200
Inductor (mH)	L	3
Switching frequency (KHz)	$f_s$	5
Resistive load ()	R	50

#### 4.MAXIMUM POWER POINT TRACKING TECHNIQUES

Control objective is to efficiently capture and harvest the utmost power of photovoltaic (PV) arrays according to the present solar radiation levels. A large number of various algorithms have been devised to locate MPP. They differ in the required use of sensors, complexity, price, scope of applicability, tracking rate, efficiency, capability of tracing radiation or temperature changes, hardware necessary and popularity. A thorough review of various MPPT algorithms, including their

mathematical formulas, working principles, and diagrams/flowcharts, can be found in [16]

.This paper focuses on two MPPT methods.

P&O: This method involves continuously adjusting the operating point of the PV system. By perturbing the voltage or current and observing the resulting power output, the system can determine how to maintain the maximum power point.

ANN: This approach utilizes the adaptive learning capabilities of neural networks to optimize the power output from PV systems.

Both methods will be explored in depth in the subsequent sections.

**4.1.P&O Method**

P&O is one of the most popular MPPT techniques of PV systems, which is easy to use and reasonably priced. The PV panel measurement's voltage (V), current (I), and initial power (P1) initiate the connection. The operating voltage is then adjusted slightly and another power reading is obtained (P2). The power change ( $\Delta P$ ) is given by the difference between P2 and P1. When  $+\Delta P$  ( $P2 > P1$ ) the perturbation is moving the system towards MPP, hence the algorithm should continue perturbing in the same direction. On the other hand, when  $-\Delta P$  ( $P2 < P1$ ) then this indicates that the perturbation has shifted beyond the MPP and the algorithm will change

direction. This cyclic procedure continues to adjust the voltage until it reaches and harvested the maximum power point of the PV panel. The overview of the P&O algorithm is presented in Table (3) [17, 18]. This technique offers several benefits, including its simplicity and widespread use. However, it does have limitations, particularly in rapidly changing atmospheric conditions or when multiple local maxima are present. Additionally, it may exhibit slow response times to the MPP and cause oscillations around the MPP. Despite these drawbacks, its easy implementation keeps it a favored option in many PV applications[19]. Figure.(6) displays a flowchart that explains the P&O MPPT technique.

**Table .(3):** Scheme of the P&O algorithm.

Present perturbation ( $\Delta V$ )	Change in power $\Delta P$	Next perturbation direction
$\Delta V > 0$	$\Delta P > 0$	Positive (Duty ratio decrease)
$\Delta V > 0$	$\Delta P < 0$	Negative (Duty ratio increase)
$\Delta V < 0$	$\Delta P > 0$	Negative (Duty ratio increase)
$\Delta V < 0$	$\Delta P < 0$	Positive (Duty ratio increase)

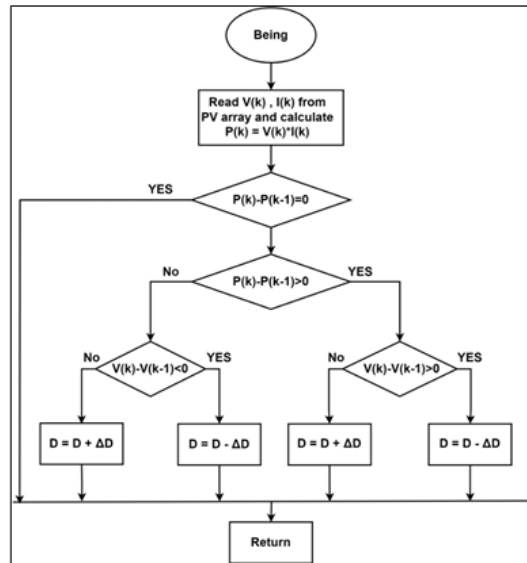


Figure. (6): flowchart of the P&O MPPT technique

4.2:ANN based MPPT

Artificial neural network controllers have become in recent years very popular to track the maximum power point in photovoltaic systems because of their ability to deal with the complex and nonlinear behavior of the system [20]. The ANN based MPPT is realized by utilizing the fact that the neural network can compute without requiring any manual programming and without requiring any learning based on data. With the highly correlated parameters being known, e.g. irradiance of the sunlight, temperature and power output, an ANN can be used to predict the

MPP and also enhance the tracking accuracy and efficiency even in various environmental situations. This is done by training the network on a dataset comprising of input, such as irradiance and temperature, as well as output expressed in terms of duty cycle values. The studies in the literature [21, 22] have considered many MPPT techniques based on ANN. The three processes involved in developing an artificial neural network (ANN) can be summed up as follow:  
 1.ANN architecture selection: The ANN architecture (depth and width of the network and the problem complexity) of the ANN is

determined by the number of layers (depth) and neurons (width) and amount of available data. Moreover, by selecting appropriate activation function (e.g., Sigmoid, Tanh or ReLU), the network would learn nonlinear relationships.

2. Collecting of data: Data collection entails putting down vital inputs and their reliable outputs. This comprises environmental conditions such as solar irradiance, temperature and the systems response such as power generation. This is the set of data points that are utilized in training the network and making it more accurate, and it is called training points.

3. Network Training and validation: Network training is performed by training the ANN with some suitable optimization algorithm, such as backpropagation using processed data. Network validation is however the process in which the accuracy and the robustness of the trained ANN are tested on another dataset.

**4.3. Choosing the ANN architecture:**

The developed neural network is a Multi-Layer Perceptron (MLP) with three layers: an input layer with two neurons (temperature and irradiance), a hidden layer with ten neurons using a sigmoid activation func-

tion, and an output layer with one neuron to determine the duty cycle using a linear activation function, as shown in Figure.(7). The network works by multiplying inputs with weights, summing them, and passing the result through the activation function to generate the output. By adjusting the weights and activation function, the network learns to recognize patterns. Equation 8 illustrates the neural network’s operation:

$$a_i = \sum_{j=0}^N W_{ij}X_j \text{---(8)}$$

Where

$a_i$  is the output of ANN at node  $i$ .

$W_{ij}$  weighted between the nodes  $i$  and  $j$ .

$X_j$  is the state variable evaluated by the activation function.

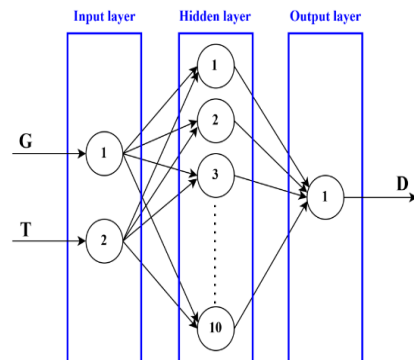


**Figure. (7):** The neural network configuration.

**5.DATA COLLECTION**

The training phase involves collecting data and outlining the steps to create a dataset for training a neural network that can predict the Duty Cycle (D) required to control the converter for optimal efficiency, based on input parameters solar irradiance (G) and temperature (T). The data collection process is illustrated in the flowchart in Fig. 8. It begins by defining the required parameters and constants, with a total of N=3000 representing the number of data samples to be generated. The temperature range is set between 5°C and 45°C (Tmin=5, Tmax=45), and the solar irradiance range is set from 10 to 1000 W/m<sup>2</sup> (Gmin=10, Gmax=1000). During each iteration, random temperature and irradiance values are generated within these ranges to ensure diversity in the dataset. The photovoltaic system is then simulated in the SIMULINK-MATLAB environment, through simulation, the maximum voltage (Vmp) and maximum power (Pmp) at the maximum power point (MPP) are obtained, these values are stored in the MATLAB workspace, and from these values, the impedance at MPP (Rmpp) is calculated using Equation 9:

$$R_{mpp} = V_{mp}^2 / P_{mp} \text{---(9)}$$

The Duty Cycle (D) is then calculated using the equation 10:

$$D = 1 - \sqrt{(R_{mpp}/R_{load})} \text{---(10)}$$

where the load resistance (Rload) is assumed to be 50 Ω.

The generated input values (G and T) and the computed duty cycle (D) are stored in matrices. The input matrix contains the values of G and T, while the output vector contains the corresponding duty cycle values. This dataset, organized as input-output pairs, is ready to be used to train the neural network. After training, the neural network will be able to predict the duty cycle based on new input values of solar irradiance and temperature, allowing for efficient real-time control of the PV system.

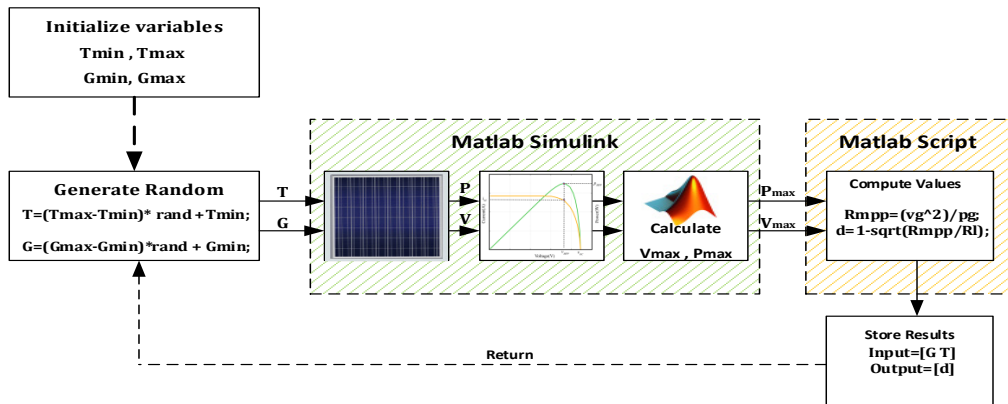


Figure. (8): Data Collection Flow Diagram

## 6.NETWORK TRAINING AND VALIDATION

An artificial neural network (ANN) was created using MATLAB’s neural network toolbox and the input/output data that had been gathered in the previous step. Depending on the availability of sensors, temperature and solar radiation were employed as input signals. To make implementation easier, the ANN’s output was defined as the boost converter’s duty cycle. The Levenberg-Marquardt algorithm was trained on a dataset of 3000 tests running under various radiation and temperature conditions. Three subsets of the data were created: 15% for testing, 15% for validation, and 70% for

training. The training process concluded after 307 epochs, as illustrated in Figure.(9). The best validation performance was achieved at epoch 301, with a mean square error (MSE) of  $1.2171e-8$ , as shown in Figure.(10). The ANN error histogram for testing, validation, and training is shown in Figure. (11). The error is separated into 20 bins with a bin width of 0.00057945, ranging from -0.00654 to 0.005045. The number of samples falling within a given error range is shown by each vertical bar. The error histogram indicates that roughly 99% of the errors fall within the range of -0.00105 to 0.000775, with a few outliers. Near the orange “Zero Error” line, the bin at -0.000165 contains over 1500 samples from the validation dataset. The

convergence of the histogram to zero across 20 bins underscores the ANN’s efficiency in achieving MPPT. This is further validated by the regression analysis shown in Figure.12, which highlights the accuracy of the ANN’s output predictions in relation to the input, with a regression value of  $R = 1$ . The error is defined as the variance between the duty cycle generated by the ANN model and the intended target duty cycle, calculated by subtracting the output from the target. As shown in the regression plot, the regression plot, the Levenberg-Marquardt (LM) algorithm was good at training the data, since the error was minimized and the output is very close to the desired values.

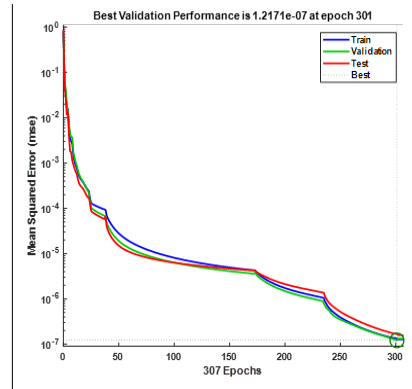


Fig. 10: Validation performance of ANN

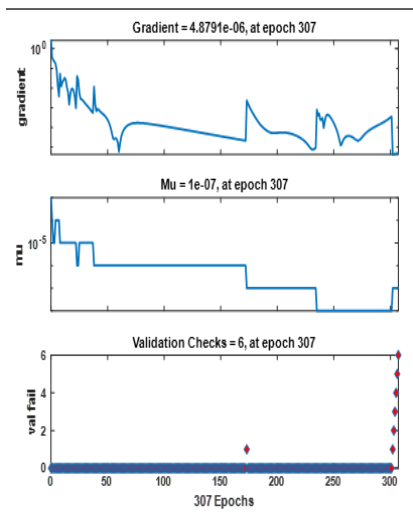


Figure. (9): Training performance of ANN

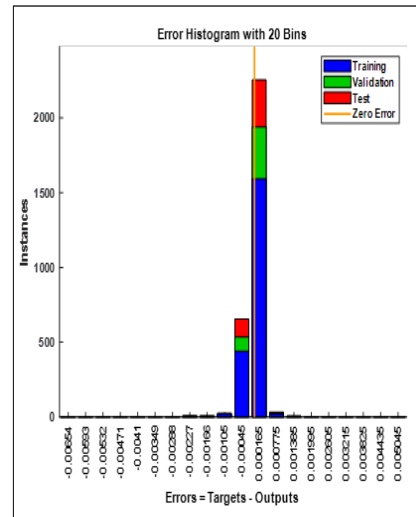


Figure. (11): Error histogram

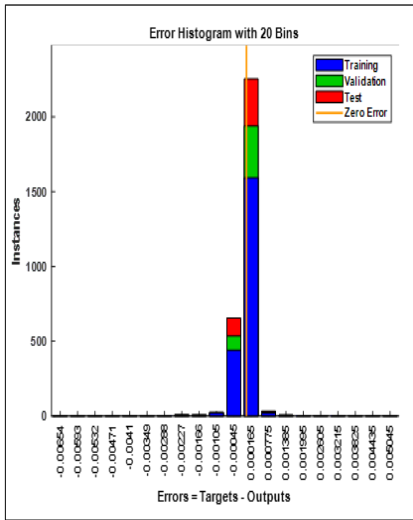


Figure. (12): Regression plot

7.RESULTS AND DISCUSSION

The simulation results of the suggested system, which was developed and analyzed using MATLAB and Simulink, are provided in this section. It is made up of load, DC-DC converter, MPPT controller, and PV arrays. Table (1) displays the PV array’s electrical properties. Two approaches have been used to evaluate the system’s performance using the P&O algorithm and an ANN-based method. Figure. (13) and Figure. (14) illustrate the design and the architecture of both approaches. Extensive testing and analysis of the solar radiation conditions AND temperature were conducted on both techniques. In addition, for a comprehensive evaluation,

a comparison is made with the previously developed FLC from our earlier work. It is important to note that the detailed results and analysis of the FLC method were extensively discussed and published in<sup>[11]</sup>; therefore, only the comparative results between FLC, P&O, and ANN methods are presented and analyzed in this section.

The simulations were conducted by dynamically varying the solar irradiance levels. Initially, the irradiance decreased from 1000 W/m<sup>2</sup> to 800 W/m<sup>2</sup> within 0.2 seconds, followed by a drop to 400 W/m<sup>2</sup> at 0.3 seconds, and then further declined to 200 W/m<sup>2</sup> at 0.7 seconds. Subsequently, it returned to the standard test condition of 1000 W/m<sup>2</sup> at 0.7 seconds, as illustrated in Fig. 15. Throughout this scenario, the ambient temperature was maintained constant at 25 °C.

In a separate scenario, the temperature variation was studied while keeping the solar irradiance fixed. The temperature increased from 15 °C to 25 °C within 0.2 seconds, then rose to 35 °C at 0.4 seconds, and finally reached 45 °C at 0.6 seconds, as shown in Fig. 16, with the irradiance held constant at 1000 W/m<sup>2</sup>.

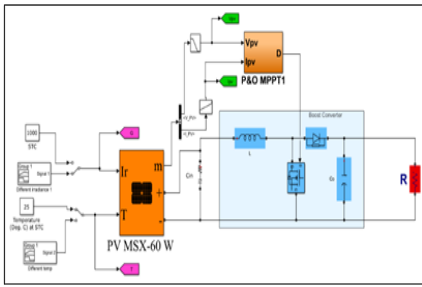


Figure. (13): Simulink Model of P&O

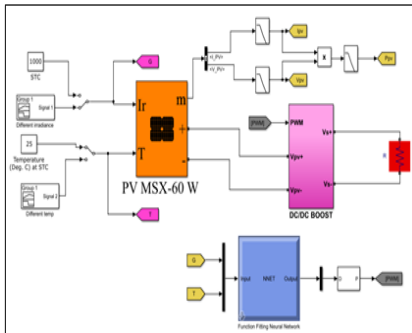


Figure. (14): Simulink Model of ANN

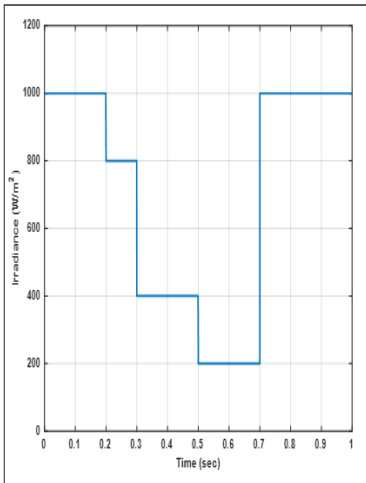


Figure. (15): Solar irradiance levels

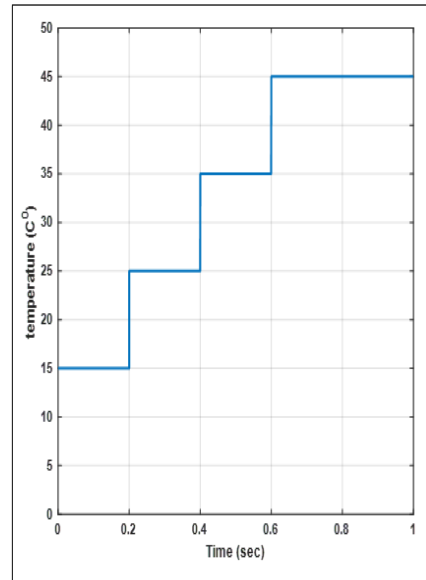


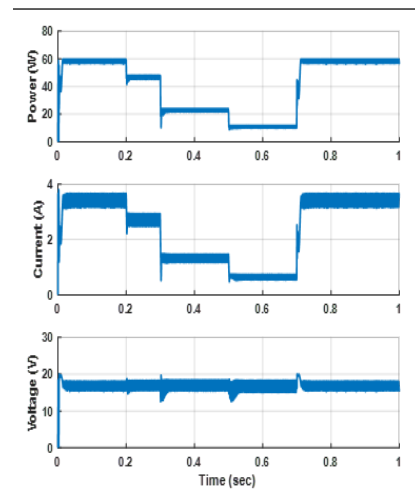
Figure. (16): Solar Temperature Variation

Figure.(17) presents the simulation results for the PV panel’s output power, current, and voltage using the P&O algorithm under dynamically changing irradiance conditions. In this setup, the duty cycle increment ( $\Delta D$ ) was set at 0.005 to ensure effective tracking of the MPP. As anticipated, a trade-off emerges between the convergence speed the time needed to reach steady state and the magnitude of oscillations around the MPP. These two characteristics are inherently linked to the value of the duty cycle increment; minimizing oscillations slows down convergence, whereas faster convergence results in larger oscillations. In this simula-

tion, the MPP was achieved in approximately 0.014 seconds at an irradiance of 1 kw/m<sup>2</sup>. Simultaneously, the effect of temperature variation at constant irradiance was also examined. Figure.(18) shows the PV panel’s output performance under gradually increasing temperature levels. Under these conditions, the MPP was reached in about 0.01 seconds at 1 kw/m<sup>2</sup> irradiance. The results indicate that although the P&O method is capable of accurately tracking the MPP, it responds relatively slowly to sudden changes in irradiance and temperature. Moreover, the method exhibits noticeable fluctuations around the optimal point, achieving a tracking efficiency of 96.2% under constant temperature conditions and 97.54% under constant irradiance at 25°C.

Figure.(19) illustrates the simulation results of the ANN-based MPPT algorithm, showing the PV panel’s output power, current, and voltage under dynamically changing irradiance conditions while maintaining a constant temperature. The ANN demonstrated excellent performance, reaching the Maximum Power Point (MPP) in just 0.008 seconds, compared to 0.014 seconds required by the P&O algorithm. Similarly,

Figure.(20) presents the ANN’s performance under varying temperature conditions at constant irradiance. The ANN method resulted in a significantly smoother power curve, exhibiting fewer fluctuations around the operating point and greater overall stability compared to the P&O method. The tracking efficiency achieved by the ANN algorithm was outstanding, reaching 99.9% across all tested irradiance and temperature variations.



**Figure. (17):** Simulation results from P&O under varying irradiance conditions

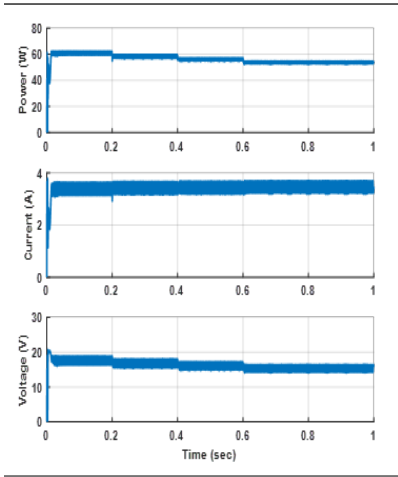


Figure. (18): Simulation results from P&O

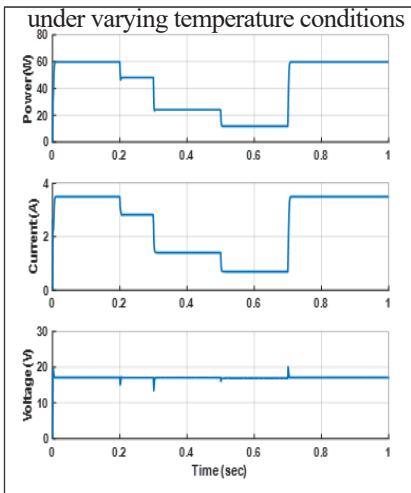


Figure. (19): Simulation results from ANN under varying irradiance conditions

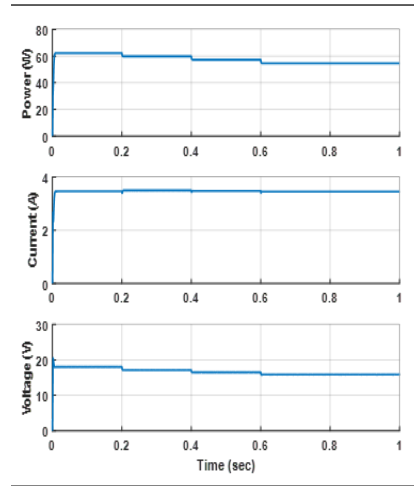
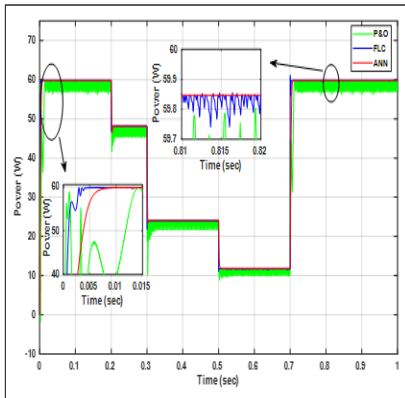


Figure. (20): Simulation results from ANN under varying temperature conditions

The tracking performance of the P&O, ANN, and previously published FLC algorithms was comparatively evaluated under varying irradiance and temperature conditions, as illustrated in Figure.(21) and Figure. (22). Table (4) presents key performance indicators including tracking efficiency, response time, and output power under different solar irradiance levels, while Table (5) summarizes the same metrics under varying temperature scenarios. The P&O method achieved dynamic tracking efficiencies of 96.20%, 97.06%, 98.88%, and 92.29% at irradiance levels of 1000 W/m<sup>2</sup>, 800 W/m<sup>2</sup>, 400 W/m<sup>2</sup>, and 200 W/m<sup>2</sup>, respectively. In contrast,

the ANN controller consistently maintained a high tracking efficiency of approximately 99.9% across all irradiance and temperature variations, demonstrating superior reliability and accuracy. Although the FLC approach reported in our earlier publication showed a faster dynamic response compared to ANN and P&O, it exhibited more noticeable power fluctuations. By comparison, the ANN-based method delivered smoother output with minimal oscillations around the maximum power point, highlighting its effectiveness for stable PV system operation.



**Figure. (21):** Output power from P&O and ANN and FLC under varying irradiance conditions

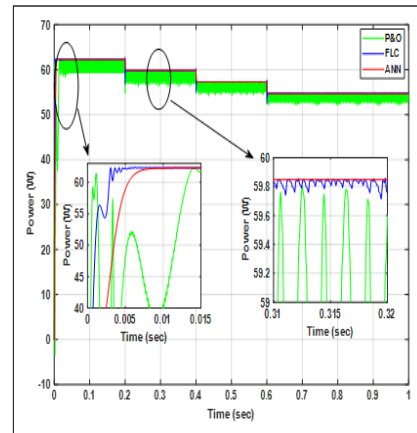


**Figure. (22):** Output power from P&O , ANN and FLC under varying temperature conditions

**Table .(4):** Comparative Analysis of ANN ,P&O and FLC MPPT Techniques under varying irradiance conditions.

Functional conditions	MPPT algorithm	Output power	Tracking efficiency	Time response
G1= 1000W/ m <sup>2</sup>	P&O	57.578	96.20%	0.014s
	FLC	59.81	99.94	0.007s
	ANN	59.84	99.98%	0.008s
G2= 800W/ m <sup>2</sup>	P&O	46.72	97.06%	0.01s
	FLC	48.10	99.92	0.004
	ANN	48.12	99.95%	0.006s
G3= 400W/ m <sup>2</sup>	P&O	23.782	98.88%	0.018s
	FLC	24.03	99.92	0.003
	ANN	24.04	99.98%	0.012s
G4= 200W/ m <sup>2</sup>	P&O	10.9	92.29%	0.01s
	FLC	11.73	99.2	0.004
	ANN	11.81	99.99%	0.006s

**Table .(5):** Comparative Analysis of ANN ,P&O and FLC MPPT Techniques under varying temperature conditions.

Functional conditions	MPPT algorithm	Output power	Tracking efficiency	Time response
T1= 15	P&O	60.66	97.33%	0.03s
	FLC	62.18	99.70%	0.005s
	ANN	62.30	99.93%	0.006s
T2= 25	P&O	58.38	97.54%	0.01s
	FLC	59.77	99.86%	0.002s
	ANN	59.85	99.99%	0.002s
T3= 35	P&O	55.87	97.45%	0.01s
	FLC	57.20	99.77%	0.003s
	ANN	57.28	99.91%	0.004s
T4= 45	P&O	53.74	98.10%	0.009s
	FLC	54.57	99.61%	0.004s
	ANN	54.68	99.81%	0.005s

## 8.CONCLUSION

A comprehensive comparative study of three MPPT controllers are presented: the classical P&O algorithm, an ANN-based controller, and a previously published FLC method. The P&O algorithm successfully tracks the MPP, but with noticeable delay and oscillations around the MPP, which are influenced by the duty cycle increment. Comparative results show that the ANN-based controller achieves superior tracking accuracy, a significantly faster transient response, and minimal steady-state power oscillations. Moreover, the Artificial Neural Network (ANN) exhibits exceptional adaptability to abrupt variations in solar irradiance and temperature, consistently maintaining a dynamic efficiency above 99.9% even under rapidly changing environmental conditions. Although the FLC method, reported in our earlier work, provides a faster initial response than ANN and P&O, it is more complex to design and tune, and suffers from greater power fluctuations around the MPP. In contrast, the ANN-based approach offers a simpler and more flexible implementation for system designers, making it a highly practical solution. In addition, this paper offers a

holistic view of MPPT control techniques, presenting a detailed analysis of their advantages, limitations, and overall performance under various operating scenarios. The study further demonstrates the potential applicability of these methods for photovoltaic system deployment in Libya, considering the differing climatic conditions between coastal cities and desert regions.

## 9.REFERENCES

- 1.Esram T, Chapman PL. Comparison of photovoltaic array maximum power point tracking techniques. *IEEE Transactions on energy conversion.* 2007;22(2):439-49.
- 2.Salas V, Olías E, Barrado A, Lazaro A. Review of the maximum power point tracking algorithms for stand-alone photovoltaic systems. *Solar energy materials and solar cells.* 2006;90(11):1555-78.
- 3.Ramos Hernanz J, Campayo Martín J, Zamora Berver I, Larranaga Lesaka J, Zulueta Guerrero E, Puelles Perez E, editors. *Modelling of photovoltaic module. International Conference on Renewable Energies and Power Quality (ICREPQ); 2010.*
- 4.Sharma C, Jain A. Maximum Power Point Tracking Techniques: A Review. *International Journal of Recent Research in Electrical*

- and Electronics Engineering (IJRREEE). 2014;1(1):25-33.
- 5.Safari A, Mekhilef S. Simulation and hardware implementation of incremental conductance MPPT with direct control method using cuk converter. IEEE transactions on industrial electronics. 2010;58(4):1154-61.
- 6.Femia N, Petrone G, Spagnuolo G, Vitelli M. Optimization of perturb and observe maximum power point tracking method. IEEE transactions on power electronics. 2005;20(4):963-73.
- 7.Al-Majidi SD, Abbod MF, Al-Raweshidy HS. A novel maximum power point tracking technique based on fuzzy logic for photovoltaic systems. International Journal of Hydrogen Energy. 2018;43(31):14158-71.
- 8.Younis MA, Khatib T, Najeeb M, Ariffin AM. An improved maximum power point tracking controller for PV systems using artificial neural network. Przegląd Elektrotechniczny. 2012;88(3b):116-21.
- 9.Hussain MT, Sarwar A, Tariq M, Urooj S, BaQais A, Hossain MA. An evaluation of ANN algorithm performance for MPPT energy harvesting in solar PV systems. Sustainability. 2023;15(14):11144.
- 10.Roy RB, Rokonuzzaman M, Amin N, Mishu MK, Alahakoon S, Rahman S, et al. A comparative performance analysis of ANN algorithms for MPPT energy harvesting in solar PV system. IEEE Access. 2021;9:102137-52.
- 11.Majdi HS. Modeling and Performance Evaluation of Incremental Conductance and Fuzzy Logic MPPT Controllers in Photovoltaic Systems.
- 12.Eid MAE, Elbaset AA, Ibrahim HA, Abdelwahab SAM, editors. Modelling, simulation of MPPT using perturb and observe and incremental conductance techniques for stand-alone PV Systems. 2019 21st International Middle East Power Systems Conference (MEPCON); 2019: IEEE.
- 13.Jazayeri M, Uysal S, Jazayeri K, editors. Evaluation of maximum power point tracking techniques in PV systems using MATLAB/Simulink. 2014 Sixth Annual IEEE Green Technologies Conference; 2014: IEEE.
- 14.Srinivasan S, Tiwari R, Krishnamoorthy M, Lalitha MP, Raj KK. Neural network based MPPT control with reconfigured quadratic boost converter for fuel cell application. International journal of hydrogen energy. 2021;46(9):6709-19.
- 15.Cheddadi Y, Errahimi F, Es-sbai N. De-

sign and verification of photovoltaic MPPT algorithm as an automotive-based embedded software. *Solar Energy*. 2018;171:414-25.

16.Ali A, Almutairi K, Padmanaban S, Tirth V, Algarni S, Irshad K, et al. Investigation of MPPT techniques under uniform and non-uniform solar irradiation condition—a retrospection. *Ieee Access*. 2020;8:127368-92.

17.Jordehi AR. Maximum power point tracking in photovoltaic (PV) systems: A review of different approaches. *Renewable and Sustainable Energy Reviews*. 2016;65:1127-38.

18.Saleh AL, Obed AA, Hassoun ZA, Yaqoob SJ, editors. Modeling and Simulation of A Low Cost Perturb& Observe and Incremental Conductance MPPT Techniques In Proteus Software Based on Flyback Converter. *IOP Conference Series: Materials Science and Engineering*; 2020: IOP Publishing.

19.Sharma D, Purohit G, editors. Advanced perturbation and observation (P&O) based maximum power point tracking (MPPT) of a solar photo-voltaic system. 2012 IEEE 5th India International Conference on Power Electronics (IICPE); 2012: IEEE.

20.Lee HH, Dzung PQ, Vu NTD, editors. The new maximum power point tracking algorithm using ANN-based solar PV systems.

TENCON 2010-2010 IEEE Region 10 Conference; 2010: IEEE.

21.Kellal C, Lakhdar M, Kouzou A, Ouacel A, editors. An ANN-based Maximum Power Point Tracking Using DC/DC Boost Converter for PV System. 2023 1st International Conference on Renewable Solutions for Ecosystems: Towards a Sustainable Energy Transition (ICRSEtoSET); 2023: IEEE.

22.Mishra SK, Sahu JK, Reddy TMPC, editors. MPPT for a Solar PV Array: ANN and P&O Comparison. 2023 IEEE 3rd International Conference on Technology, Engineering, Management for Societal impact using Marketing, Entrepreneurship and Talent (TEMSMET); 2023: IEEE.